Theoretical Prediction of the Fractional ac Josephson Effect in p- and d-Wave Superconductors

Hyok-Jon Kwon,[1] K. Sengupta,[2] and Victor M. Yakovenko[1]

[1]*Department of Physics, University of Maryland, College Park, Maryland 20742-4111, USA*

[2]*Department of Physics, Yale University, New Haven, Connecticut 06520-8120, USA*

Received on 23 May, 2003.

For certain orientations of Josephson junctions between two p_x-wave or two d-wave superconductors, the subgap Andreev states produce a 4π-periodic relation between the Josephson current I and the phase difference ϕ: $I \propto \sin(\phi/2)$. Consequently, the ac Josephson current has the fractional frequency $eV/\hbar$, where V is the dc voltage. In the tunneling limit, the Josephson current is proportional to the first power (not square) of the electron tunneling amplitude. Thus, the Josephson current is carried by single electrons, rather than by Cooper pairs.

1 Introduction

In many materials, the symmetry of the superconducting order parameter is unconventional, i.e. not s-wave. In the high-T_c cuprates, it is the singlet $d_{x^2-y^2}$-wave [1]. There is experimental evidence that, in the quasi-one-dimensional (Q1D) organic superconductors $(\mathrm{TMTSF})_2\mathrm{X}$ [2], the symmetry is triplet [3], most likely the p_x-wave [4], with the x axis is along the conducting chains. The unconventional pairing symmetry typically results in formation of subgap Andreev bound states on the surfaces of these superconductors. For d-wave cuprate superconductors, the midgap Andreev states were predicted theoretically in Ref. [5] and discovered experimentally as a zero-bias conductance peak in tunneling between normal metals and superconductors (see review [6]). For the Q1D organic superconductors, the midgap states were theoretically predicted to exist at the edges perpendicular to the chains [7, 8]. When two unconventional superconductors are joined together in a Josephson junction, their Andreev surface states hybridize to form Andreev bound states in the junction. These states are important for the Josephson current. Andreev bound states in high-T_c junctions were reviewed in Ref. [9]. The Josephson effect between two Q1D p-wave superconductors was studied in Refs. [10, 11].

In the present paper, we predict a new effect for Josephson junctions between unconventional nonchiral superconductors, which we call the fractional ac Josephson effect. Suppose both superconductors forming a Josephson junction have surface midgap states originally. This is the case for the butt-to-butt junction between two p_x-wave Q1D superconductors, as shown in Fig. 1a, and for the $45°/45°$ in-plane junction between two d-wave superconductors, as shown in Fig. 2a. (The two angles indicate the orientation of the junction line relative to the $\mathbf{b}$ axes of each $d_{x^2-y^2}$ superconductor.) We predict that the contribution of the hybridized Andreev bound states produces a 4π-periodic relation between the supercurrent I and the superconducting phase difference ϕ: $I \propto \sin(\phi/2)$ [12]. Consequently, the ac Josephson effect has the frequency $eV/\hbar$, where e is the electron charge, V is the applied dc voltage, and $\hbar$ is the Planck constant. The predicted frequency is a half of the conventional Josephson frequency $2eV/\hbar$ originating from the conventional Josephson relation $I \propto \sin\phi$ with the period of 2π. Qualitatively, the predicted effect can be understood as follows. The Josephson current across the two unconventional superconductors is carried by tunneling of *single electrons* (rather than Cooper pairs) between the two resonant midgap states. Thus, the Cooper pair charge $2e$ is replaced the single charge e in the expression for the Josephson frequency. This interpretation is also supported by the finding that, in the tunneling limit, the Josephson current is proportional to the first power (not square) of the electron tunneling amplitude [13]. Possibilities for experimental observation of the fractional ac Josephson effect are discussed in Sec. 5.

The predicted current-phase relation $I \propto \sin(\phi/2)$ is quite radical, because every textbook on superconductivity says that the Josephson current must be a 2π-periodic function of ϕ [12]. To our knowledge, the only paper that discussed the 4π-periodic Josephson effect is Ref. [14] by Kitaev. He considered a highly idealized model of spinless fermions on a one-dimensional (1D) lattice with superconducting pairing on the neighboring sites. The pairing potential in this case has the p_x-wave symmetry, and midgap states exist at the ends of the chain. They are described by the Majorana fermions, which Kitaev proposed to use for nonvolatile memory in quantum computing. He found that, when two such superconductors are brought in contact, the system is 4π-periodic in the phase difference between the superconductors. Our results are in agreement with his work. However, we formulate the problem as an experimentally realistic Josephson effect between known superconducting materials.

2 The basics

We consider the case where the spin polarization vector $\mathbf{n}$ of the triplet pairing has a uniform, momentum-independent orientation [3, 4]. If the spin quantization axis z is selected along $\mathbf{n}$, then the Cooper pairing takes place between electrons with the opposite z-axis spin projections σ and $\bar{\sigma}$: $\langle \hat{c}_\sigma(\mathbf{k})\hat{c}_{\bar{\sigma}}(-\mathbf{k})\rangle \propto \Delta_\sigma(\mathbf{k})$, where $\hat{c}_\sigma(\mathbf{k})$ is the annihilation operator of an electron with momentum $\mathbf{k}$ and spin σ. The pairing potential has the symmetry $\Delta_\sigma(\mathbf{k}) = \mp\Delta_{\bar{\sigma}}(\mathbf{k}) = \pm\Delta_\sigma(-\mathbf{k})$, where the upper and lower signs correspond to the singlet and triplet cases.

We select the coordinate axis x perpendicular to the Josephson junction plane. We assume that the interface between the two superconductors is smooth enough, so that the electron momentum component k_y parallel to the junction plane is a conserved good quantum number.

Electron states in a superconductor are described by the Bogoliubov operators $\hat{\gamma}$, which are related to the electron operators $\hat{c}$ by the following equations [15]

$$\hat{\gamma}_{n\sigma k_y} = \int dx\,[u^*_{n\sigma k_y}(x)\,\hat{c}_{\sigma k_y}(x) + v^*_{n\sigma k_y}(x)\,\hat{c}^\dagger_{\bar{\sigma}\bar{k}_y}(x)], \tag{1}$$

$$\hat{c}_{\sigma k_y}(x) = \sum_n [u_{n\sigma k_y}(x)\,\hat{\gamma}_{n\sigma k_y} + v^*_{n\bar{\sigma}\bar{k}_y}(x)\,\hat{\gamma}^\dagger_{n\bar{\sigma}\bar{k}_y}], \tag{2}$$

where $\bar{k}_y = -k_y$, and n is the quantum number of the Bogoliubov eigenstates. The two-components vectors $\psi_{n\sigma k_y}(x) = [u_{n\sigma k_y}(x), v_{n\sigma k_y}(x)]$ are the eigenstates of the Bogoliubov-de Gennes (BdG) equation with the eigenenergies $E_{n\sigma k_y}$:

$$\begin{pmatrix} \varepsilon_{k_y}(\hat{k}_x) + U(x) & \hat{\Delta}_{\sigma k_y}(x,\hat{k}_x) \\ \hat{\Delta}^\dagger_{\sigma k_y}(x,\hat{k}_x) & -\varepsilon_{k_y}(\hat{k}_x) - U(x) \end{pmatrix} \psi_n = E_n \psi_n, \tag{3}$$

where $\hat{k}_x = -i\partial_x$ is the x component of the electron momentum operator, and $U(x)$ is a potential. In Eq. (3) and below, we often omit the indices σ and k_y to shorten notation where it does not cause confusion.

3 Junctions between quasi-one-dimensional superconductors

In this section, we consider junctions between two Q1D superconductors, such as organic superconductors $(\mathrm{TMTSF})_2\mathrm{X}$, with the chains along the x axis, as shown in Fig. 1a. For a Q1D conductor, the electron energy dispersion in Eq. (3) can be written as $\varepsilon = \hbar^2\hat{k}_x^2/2m - 2t_b\cos(bk_y) - \mu$, where m is an effective mass, μ is the chemical potential, b and t_b are the distance and the tunneling amplitude between the chains. The superconducting pairing potentials in the s- and p_x-wave cases have the forms

$$\hat{\Delta}_{\sigma k_y}(x,\hat{k}_x) = \begin{cases} \sigma\Delta_\beta, & s\text{-wave}, \\ \Delta_\beta\,\hat{k}_x/k_F, & p_x\text{-wave}, \end{cases} \tag{4}$$

where $\hbar k_F = \sqrt{2m\mu}$ is the Fermi momentum, and σ is treated as $+$ for $\uparrow$ and $-$ for $\downarrow$. The index $\beta = R, L$ labels the right ($x > 0$) and left ($x < 0$) sides of the junction, and Δ_β acquires a phase difference ϕ across the junction:

$$\Delta_R = \Delta_0 e^{i\phi}, \qquad \Delta_L = \Delta_0\,. \tag{5}$$

The potential $U(x) = U_0\delta(x)$ in Eq. (3) represents the junction barrier located at $x = 0$. Integrating Eq. (3) over x from –0 to +0, we find the boundary conditions at $x = 0$:

$$\psi_L = \psi_R, \quad \partial_x\psi_R - \partial_x\psi_L = k_F Z\,\psi(0), \tag{6}$$

$$Z = 2mU_0/\hbar^2 k_F, \quad D = 4/(Z^2+4), \tag{7}$$

where D is the transmission coefficient of the barrier.

A. Andreev bound states

A general solution of Eq. (3) is a superposition of the terms with the momenta close to αk_F, where the index $\alpha = \pm$ labels the right- and left-moving electrons:

$$\psi_{\beta\sigma} = e^{\beta\kappa x}\left[A_\beta \begin{pmatrix} u_{\beta\sigma+} \\ v_{\beta\sigma+} \end{pmatrix} e^{i\tilde{k}_F x} + B_\beta \begin{pmatrix} u_{\beta\sigma-} \\ v_{\beta\sigma-} \end{pmatrix} e^{-i\tilde{k}_F x}\right]. \tag{8}$$

Here $\beta = \mp$ for R and L. Eq. (8) describes a subgap state with an energy $|E| < \Delta_0$, which is localized at the junction and decays exponentially in x within the length $1/\kappa$. The coefficients $(u_{\beta\sigma\alpha}, v_{\beta\sigma\alpha})$ in Eq. (8) are determined by substituting the right- and left-moving terms separately into Eq. (3) for $x \neq 0$, where $U(x) = 0$. In the limit $k_F \gg \kappa$, we find

$$\frac{u_{\beta\sigma\alpha}}{v_{\beta\sigma\alpha}} = \frac{\Delta_{\beta\sigma\alpha}}{E + i\alpha\beta\hbar\kappa v_F}, \quad \kappa = \frac{\sqrt{\Delta_0^2 - |E|^2}}{\hbar v_F}, \tag{9}$$

where $v_F = \hbar k_F/m$ is the Fermi velocity, and $\Delta_{\beta\sigma\alpha}$ is equal to $\sigma\Delta_\beta$ for s-wave and to $\alpha\Delta_\beta$ for p_x-wave, with Δ_β given by Eq. (5). The k_y-dependent Fermi momentum $\hbar\tilde{k}_F = \hbar k_F + 2t_b\cos(bk_y)/v_F$ in Eq. (8) eliminates the dispersion in k_y from the BdG equation.

Substituting Eq. (8) into the boundary conditions (6), we obtain the linear homogeneous equations for the coefficients A_β and B_β. The compatibility condition for these equations gives an equation for the energies of the Andreev bound states. There are two subgap states with the energies $E_a = aE_0(\phi)$ labeled by the index $a = \pm$:

$$E_0^{(s)}(\phi) = -\Delta_0\sqrt{1 - D\sin^2(\phi/2)}, \quad s\text{-}s \text{ junction}, \tag{10}$$

$$E_0^{(p)}(\phi) = -\Delta_0\sqrt{D}\cos(\phi/2), \quad p_x\text{-}p_x \text{ junction}. \tag{11}$$

The energies (10) and (11) are plotted as functions of ϕ in the left panels (b) and (c) of Fig. 1. Without barrier ($D = 1$), the spectra of the s-s and p_x-p_x junctions are the same and consist of two crossing curves $E = \mp\Delta_0 \cos\phi/2$, shown by the thin lines in the left panel of Fig. 1b. A nonzero barrier ($D < 1$) changes the energies of the Andreev bound states in the s-s and p_x-p_x junctions in different ways. In the s-s case, the two energy levels repel near $\phi = \pi$ and form two separated 2π-periodic branches shown by the thick lines in the left panel of Fig. 1b [15, 16]. In contrast, in the p_x-p_x case, the two energy levels continue to cross at $\phi = \pi$, and they separate from the continuum of states above $+\Delta_0$ and below $-\Delta_0$, as show in the left panel of Fig. 1c. The absence of energy levels repulsion indicates that there is no matrix element between these levels at $\phi = \pi$ in the p_x-p_x case, unlike in the s-s case.

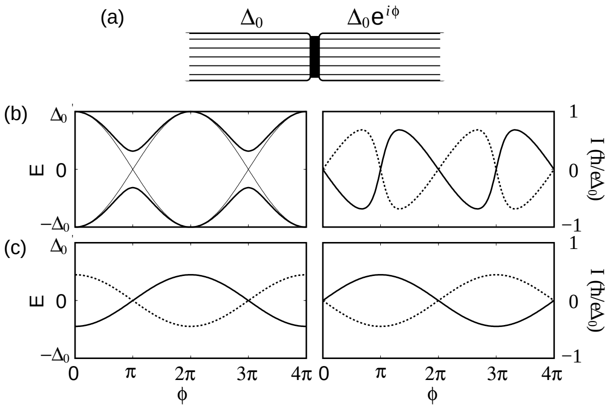

Figure 1. (a) Josephson junction between two Q1D p_x-wave superconductors. (b) The energies (left panel) and the currents (right panel) of the subgap states in the s-s junction as functions of the phase difference ϕ for $D = 1$ (thin lines) and $D = 0.9$ (thick lines). (c) The same as (b) for the p_x-p_x junction at $D = 0.2$.

As shown in Sec. 4, the $45°/45°$ junction between two d-wave superconductors is mathematically equivalent to the p_x-p_x junction. Eq. (11) was derived for the $45°/45°$ junction in Ref. [13].

B. Fractional ac Josephson effect

It is well known [15] that the current carried by a quasiparticle state a is

$$I_a = \frac{2e}{\hbar}\frac{\partial E_a}{\partial \phi}. \tag{12}$$

The two subgap states carry opposite currents, which are plotted vs. ϕ in the right panels (b) and (c) of Fig. 1 for the s-s and p_x-p_x junctions. At zero temperature, only the subgap state with the lower energy is occupied in the s-s junction. Substituting Eq. (10) into Eq. (12), we recover the conventional formula for the Josephson current in the tunneling limit $D \ll 1$ for the s-s junction:

$$I_s \approx \frac{De\Delta_0}{2\hbar}\sin\phi. \tag{13}$$

Now let us consider the p_x-p_x junction at zero temperature in the initial state $\phi = 0$, where the two subgap states (11) with the energies $\pm E_0^{(p)}$ are, correspondingly, occupied and empty. Suppose a small voltage $eV \ll \Delta_0$ is applied to the junction, so the phase difference acquires dependence on time t: $\phi(t) = 2eVt/\hbar$. If $\phi(t)$ changes sufficiently slowly (adiabatically), the occupation numbers of the subgap states do not change. In other words, the states shown by the solid and dotted lines in Fig. 1c remains, correspondingly, occupied and empty. The occupied state (11) produces the current (12):

$$I_p(t) = \frac{\sqrt{D}e\Delta_0}{\hbar}\sin\left(\frac{\phi(t)}{2}\right) = \frac{\sqrt{D}e\Delta_0}{\hbar}\sin\left(\frac{eVt}{\hbar}\right). \tag{14}$$

The frequency of the ac current (14) is $eV/\hbar$, a half of the conventional Josephson frequency $2eV/\hbar$. This can be traced to the fact that the energies Eq. (11) and the corresponding wave functions have the period 4π in ϕ, rather than conventional 2π.

The 4π periodicity is the consequence of the energy levels crossing at $\phi = \pi$. (In contrast, in the s-wave case, the levels repel at $\phi = \pi$ in Fig. 1b, thus the energy curves are 2π-periodic.) As discussed at the end of Sec. 3, there is no matrix element between the energy levels at $\phi = \pi$. Thus, there are no transitions between them, so the occupation numbers of the solid and dotted curves in Fig. 1c are preserved. To show this more formally, we can write a general solution of the time-dependent BdG equation as a superposition of the two subgap states with the time-dependent $\phi(t)$: $\psi(t) = \sum_a C_a(t)\,\psi_a[\phi(t)]$. The matrix element of transitions between the states is proportional to $\dot\phi\langle\psi_+|\partial_\phi\psi_-\rangle = \dot\phi\langle\psi_+|\partial_\phi\hat H|\psi_-\rangle/(E_- - E_+)$. We found that it is zero in the p_x-wave case, thus there are no transitions, and the initial occupation numbers of the subgap states at $\phi = 0$ are preserved dynamically.

As one can see in Fig. 1c, the system is not in the ground state when $\pi < \phi < 3\pi$, because the upper energy level is occupied and the lower one is empty. In principle, the system might be able to relax to the ground state by emitting a phonon or a photon. We do not have an estimate for such inelastic relaxations time, but we expect that it is quite long. To observe the ac Josephson effect with the frequency $eV/\hbar$, the period of Josephson oscillations should be set shorter than the inelastic relaxations time, but not too short, so that the time-dependent BdG equation can be treated adiabatically.

C. Tunneling Hamiltonian approach

In the infinite barrier limit $D \to 0$, the energies $\pm E_0^{(p)}$ of the two subgap states (11) degenerate to zero, i.e. they become midgap states. The wave functions (8) simplify as follows:

$$\psi_{\pm 0} = [\psi_{L0}(x) \mp \psi_{R0}(x)]/\sqrt{2}, \tag{15}$$

$$\psi_{L0} = \sqrt{2\kappa}\,\sin(k_F x)\,e^{\kappa x}\begin{pmatrix}1\\ i\end{pmatrix}\theta(-x), \tag{16}$$

$$\psi_{R0} = \sqrt{2\kappa}\,\sin(k_F x)\,e^{-\kappa x}\begin{pmatrix}e^{i\phi/2}\\ -ie^{-i\phi/2}\end{pmatrix}\theta(x). \tag{17}$$

Since at $D = 0$ the Josephson junction consists of two semi-infinite uncoupled p_x-wave superconductors, ψ_{L0} and ψ_{R0} are the wave functions of the surface midgap states [7] belonging to the left and right superconductor. Let us examine the properties of the midgap states.

If (u, v) is an eigenvector of Eq. (3) with an eigenvalue E_n, then $(-v^*, u^*)$ for s-wave and (v^*, u^*) for p-wave are the eigenvectors with the energy $E_{\bar{n}} = -E_n$. It follows from this relation and Eq. (1) that $\hat{\gamma}^\dagger_{n\sigma k_y} = C\hat{\gamma}_{\bar{n}\bar{\sigma}\bar{k}_y}$ with $|C| = 1$. Notice that in the s-wave case, because (u, v) and $(-v^*, u^*)$ are orthogonal for any u and v, the states n and $\bar{n}$ are always different. However, in the p-wave case, the vectors (u, v) and (v^*, u^*) may be proportional, in which case they describe the same state with $E = 0$. The states (16) and (17) indeed have this property:

$$v_{L0} = iu^*_{L0}, \qquad v_{R0} = -iu^*_{R0}. \tag{18}$$

Substituting Eq. (18) into Eq. (1), we find the Bogoliubov operators of the left and right midgap states

$$\hat{\gamma}^\dagger_{L0\sigma k_y} = i\hat{\gamma}_{L0\bar{\sigma}\bar{k}_y}, \quad \hat{\gamma}^\dagger_{R0\sigma k_y} = -i\hat{\gamma}_{R0\bar{\sigma}\bar{k}_y}. \tag{19}$$

Operators (19) correspond to the Majorana fermions discussed in Ref. [14]. In the presence of a midgap state, the sum over n in Eq. (2) should be understood as $\sum_{n>0} + (1/2)\sum_{n=0}$, where we identify the second term as the projection $\mathcal{P}\hat{c}$ of the electron operator $\hat{c}$ onto the midgap state. Using Eqs. (18), (19), and (2), we find

$$\mathcal{P}\hat{c}_{\sigma k_y}(x) = u_0(x)\hat{\gamma}_{0\sigma k_y} = v^*_0(x)\hat{\gamma}^\dagger_{0\bar{\sigma}\bar{k}_y}. \tag{20}$$

Let us consider two semi-infinite p_x-wave superconductors on a 1D lattice with the spacing l, one occupying $x \le \bar{l} = -l$ and another $x \ge l$. They are coupled by the tunneling matrix element τ between the sites $\bar{l}$ and l:

$$\hat{H}_\tau = \tau \sum_{\sigma k_y} [\hat{c}^\dagger_{L\sigma k_y}(\bar{l})\,\hat{c}_{R\sigma k_y}(l) + \hat{c}^\dagger_{R\sigma k_y}(l)\,\hat{c}_{L\sigma k_y}(\bar{l})]. \tag{21}$$

In the absence of coupling ($\tau = 0$), the subgap wave functions of each superconductor are given by Eqs. (16) and (17). Using Eqs. (20), (18), (16), and (17), the tunneling Hamiltonian projected onto the basis of midgap states is

$$\begin{aligned}\mathcal{P}\hat{H}_\tau &= \tau\,[u^*_{L0}(\bar{l})u_{R0}(l) + \text{c.c.}]\,(\hat{\gamma}^\dagger_{L0\uparrow}\hat{\gamma}_{R0\uparrow} + \text{H.c.}) \\ &= \Delta_0\sqrt{D}\,\cos(\phi/2)\,(\hat{\gamma}^\dagger_{L0\uparrow}\hat{\gamma}_{R0\uparrow} + \hat{\gamma}^\dagger_{R0\uparrow}\hat{\gamma}_{L0\uparrow}),\end{aligned} \tag{22}$$

where $\sqrt{D} = 4\tau\sin^2 k_F l/\hbar v_F$ is the transmission amplitude, and we omitted summation over the diagonal index k_y. Notice that Eq. (22) is 4π-periodic in ϕ [14].

Hamiltonian (22) operates between the two degenerate states of the system related by annihilation of the Bogoliubov quasiparticle in the right midgap state and its creation in the left midgap state. In this basis, Hamiltonian (22) can be written as a 2×2 matrix

$$\mathcal{P}\hat{H}_\tau = \Delta_0\sqrt{D}\cos(\phi/2)\begin{pmatrix} 0 & 1 \\ 1 & 0 \end{pmatrix}. \tag{23}$$

The eigenvectors of Hamiltonian (23) are $(1, \mp 1)$, i.e. the antisymmetric and symmetric combinations of the right and left midgap states given in Eq. (15). Their eigenenergies are $E_\pm(\phi) = \mp\Delta_0\sqrt{D}\cos(\phi/2)$, in agreement with Eq. (11). The tunneling current operator is obtained by differentiating Eqs. (22) or (23) with respect to ϕ. Because ϕ appears only in the prefactor, the operator structures of the current operator and the Hamiltonian are the same, so they are diagonal in the same basis. Thus, the energy eigenstates are simultaneously the eigenstates of the current operator with the eigenvalues $I_\pm = \pm(\sqrt{D}e\Delta_0/\hbar)\sin(\phi/2)$, in agreement with Eq. (14). The same basis $(1, \mp 1)$ diagonalizes Hamiltonian (23) even when a voltage V is applied and the phase ϕ is time-dependent. Then the initially populated eigenstate produces the current $I_p = \sqrt{D}(e\Delta_0/\hbar)\sin(eVt/\hbar)$ with the fractional Josephson frequency $eV/\hbar$, in agreement with Eq. (14).

D. Josephson current carried by single electrons, rather than Cooper pairs

In the tunneling limit, the transmission coefficient D is proportional to the square of the electron tunneling amplitude τ: $D \propto \tau^2$. Eq. (14) show that the Josephson current in the p_x-p_x junction is proportional to the first power of τ. This is in contrast to the s-s junction, where the Josephson current (13) is proportional to τ^2. This difference results in the big ratio $I_p/I_s = 2/\sqrt{D}$ between the critical currents in the p_x- and s-wave cases. The reason for the different powers of τ is the following. In the p_x-wave case, the transfer of just one electron between the degenerate left and right midgap states is a real (nonvirtual) process. Thus, the eigenenergies are determined from the secular equation (23) already in the first order of τ. In the s-wave case, there are no midgap states, so the transferred electron is taken from below the gap and placed above the gap, at the energy cost $2\Delta_0$. Thus, the transfer of a single electron is a virtual (not real) process. It must be followed by the transfer of another electron, so that the pair of electrons is absorbed into the condensate. This gives the current proportional to τ^2. This picture implies that the Josephson supercurrent is carried by single electrons in the p_x-p_x junction and by Cooper pairs in the s-s junction. Because the single-electron charge e is a half of the Cooper-pair charge $2e$, the frequency of the ac Josephson effect in the p_x-p_x junction is $eV/\hbar$, a half of the conventional Josephson frequency $2eV/\hbar$ for the s-s junction. These conclusions also apply to a junction between two d-wave superconductors in such orientation that both sides of the junction have surface midgap states, e.g. to the $45°/45°$ junction.

4 Josephson junctions between d-wave superconductors

In this section, we study Josephson junctions between two d-wave cuprate superconductors. As before, we select the coordinate x perpendicular to the junction line and assume that the electron momentum component k_y parallel to the junction line is a conserved good quantum number. Then, the 2D problem separates into a set of 1D solutions (8) in the x direction labeled by the index k_y. Using an isotropic electron energy dispersion law $\varepsilon = \hbar^2(k_x^2 + k_y^2)/2m - \mu$, we replace the Fermi momentum k_F and velocity v_F by their x-components $k_{Fx} = \sqrt{k_F^2 - k_y^2}$ and $v_{Fx} = \hbar k_{Fx}/m$. Thus, the transmission coefficient D in Eq. (7) becomes k_y-dependent. The total Josephson current is given by a sum over all occupied subgap states labeled by k_y.

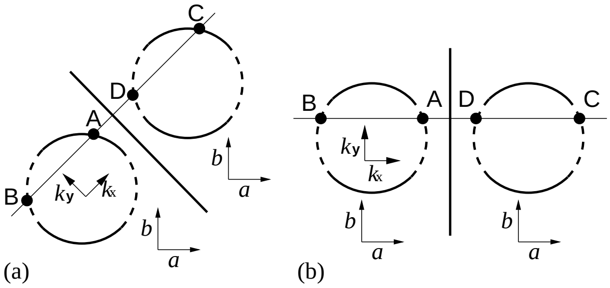

Figure 2. Schematic drawing of the $45°/45°$ junction (panel a) and $0°/0°$ junction (panel b) between two d-wave superconductors. The thick line represents the junction line. The circles illustrate the Fermi surfaces, where positive and negative pairing potentials Δ are shown by the solid and dotted lines. The points A, B, C, and D in the momentum space are connected by transmission and reflection from the barrier.

For the cuprates, let us consider a junction parallel to the $[1, \bar{1}]$ crystal direction in the a-b plane and select the x axis along the diagonal $[1, 1]$, as shown in Fig. 2a. In these coordinates, the d-wave pairing potential is

$$\hat{\Delta}_{\sigma k_y}(x, \hat{k}_x) = \sigma 2\Delta_\beta \, k_y \hat{k}_x / k_F^2, \tag{24}$$

where the same notation as in Eq. (4) is used. Direct comparison of Eqs. (24) and (4) demonstrates that the d-wave superconductor with the $45°$ junction maps to the p_x-wave superconductor by the substitution $\Delta_0 \to \sigma 2\Delta_0 k_y/k_F$. Thus, the results obtained in Sec. 3 for the p_x-p_x junction apply to the $45°/45°$ junction between two d-wave superconductors with the appropriate integration over k_y. The energies and the wave functions of the subgap Andreev states in the $45°/45°$ junction are 4π-periodic, as in Eqs. (11). Thus the ac Josephson current has the fractional frequency $eV/\hbar$, as in Eq. (14).

On the other hand, if the junction is parallel to the $[0, 1]$ crystal direction, as shown in Fig. 2b, then $\hat{\Delta}_{\sigma k_y}(x, \hat{k}_x) = \sigma\Delta_\beta \, (\hat{k}_x^2 - k_y^2)/k_F^2$. This pairing potential is an even function of $\hat{k}_x$, thus it is analogous to the s-wave pairing potential in Eq. (4). Thus, the $0°/0°$ junction between two d-wave superconductors is analogous to the s-s junction. It should exhibit the conventional 2π-periodic Josephson effect with the frequency $2eV/\hbar$.

For a generic orientation of the junction line, the d-wave pairing potential acts like p_x-wave for some momenta k_y and like s-wave for other k_y. Thus, the total Josephson current is a sum of the unconventional and conventional terms [12]:

$$I = C_1 \sin(\phi/2) + C_2 \sin(\phi) + \dots\,, \tag{25}$$

with some coefficients C_1 and C_2. We expect that both terms in Eq. (25) are present for any real junction between d-wave superconductors because of imperfections. However, the ratio C_1/C_2 should be maximal for the junction shown in Fig. 2a and minimal for the junction shown in Fig. 2b.

5 Experimental observation of the fractional ac Josephson effect

Conceptually, the setup for experimental observation of the fractional ac Josephson effect is very straightforward. One should apply a dc voltage V to the junction and measure frequency spectrum of microwave radiation from the junction, expecting to detect a peak at the fractional frequency $eV/\hbar$. Josephson radiation at the conventional frequency $2eV/\hbar$ was first observed experimentally almost 40 years ago in Kharkov [17, 18], followed by further work [19, 20]. In Ref. [18], the spectrum of microwave radiation from tin junctions was measured, and a sharp peak at the frequency $2eV/\hbar$ was found. Without any attempt to match impedances of the junction and waveguide, Dmitrenko and Yanson [18] found the signal several hundred times stronger than the noise and the ratio of linewidth to the Josephson frequency less than 10^{-3}. More recently, a peak of Josephson radiation was observed in Ref. [21] in indium junctions at the frequency 9 GHz with the width 36 MHz. In Ref. [22], a peak of Josephson radiation was observed around 11 GHz with the width 50 MHz in $\mathrm{Bi_2Sr_2CaCu_2O_8}$ single crystals with the current along the $\mathbf{c}$ axis perpendicular to the layers.

To observe the fractional ac Josephson effect predicted in this paper, all it takes is to perform the same experiment with the $45°/45°$ cuprate junctions shown in Fig. 2(a). For control purposes, it is also desirable to measure frequency spectrum for the $0°/0°$ junction shown in Fig. 2(b), where a peak at the frequency $eV/\hbar$ should be minimal. It should be absent completely in a conventional s-s junction, unless the junction enters a chaotic regime with period doubling [23]. The high-T_c junctions of the required geometry can be manufactured using the step-edge technique. Bicrystal junctions are not appropriate, because the crystal axes $\mathbf{a}$ and $\mathbf{b}$ of the two superconductors are rotated relative to each other in such junctions. As shown in Fig. 2(a), we need the junction where the crystal axes of the two superconductors have the same orientation. Unfortunately, attempts to manufacture Josephson junctions from the Q1D organic superconductors $\mathrm{(TMTSF)_2X}$ failed thus far.

The most common way of studying the ac Josephson effect is observation of the Shapiro steps. In this setup, the Josephson junction is irradiated by microwaves with the frequency ω, and steps in dc current are detected at the dc voltages $V_n = n\hbar\omega/2e$. Unfortunately, this method is not very useful to study the effect that we predict. Indeed, our results are effectively obtained by the substitution $2e \to e$. Thus, we expect to see the Shapiro steps at the voltages $V_m = m\hbar\omega/e = 2m\hbar\omega/2e$, i.e. we expect to see only *even* Shapiro steps. However, when both terms are present in Eq. (25), they produce both even and odd Shapiro steps, so it would be difficult to differentiate the novel effect from the conventional Shapiro effect. Notice also that the so-called fractional Shapiro steps observed at the voltage $V_{1/2} = \hbar\omega/4e$ corresponding to $n = 1/2$ have nothing to do with the effect that we propose. They originate from the higher harmonics in the current-phase relation $I \propto \sin(2\phi)$. The fractional Shapiro steps have been observed in cuprates [24], but also in conventional s-wave superconductors [25]. Another method of measuring the current-phase relation in cuprates was employed in Ref. [26], but connection with our theoretical results is not clear at the moment.

6 Conclusions

In this paper, we study suitably oriented p_x-p_x or d-d Josephson junctions, where the superconductors on both sides of the junction originally have the surface Andreev midgap states. In such junctions, the Josephson current I, carried by the hybridized subgap Andreev bound states, is a 4π-periodic function of the phase difference ϕ: $I \propto \sin(\phi/2)$, in agreement with Ref. [14]. Thus, the ac Josephson current should exhibit the fractional frequency $eV/\hbar$, a half of the conventional Josephson frequency $2eV/\hbar$. In the tunneling limit, the Josephson current is proportional to the first power of the electron tunneling amplitude, not the square as in the conventional case [13]. Thus, the Josephson current in the considered case is carried by single electrons with charge e, rather than by Copper pairs with charge $2e$. The fractional ac Josephson effect can be observed experimentally by measuring frequency spectrum of microwave radiation from the junction and detecting a peak at $eV/\hbar$.

The work was supported by NSF Grant DMR-0137726. KS thanks S. M. Girvin for support.

References

[1] D. J. Van Harlingen, Rev. Mod. Phys. **67**, 515 (1995); C. Tsuei and J. Kirtley, *ibid.* **72**, 969 (2000).

[2] TMTSF stands for tetramethyltetraselenafulvalene, and X represents inorganic anions such as $\mathrm{ClO_4}$ or $\mathrm{PF_6}$.

[3] I. J. Lee *et al.*, Phys. Rev. Lett. **88**, 017004 (2002); I. J. Lee, M. J. Naughton, G. M. Danner, and P. M. Chaikin, *ibid.* **78**, 3555 (1997); I. J. Lee, P. M. Chaikin, and M. J. Naughton, Phys. Rev. B **62**, R14669 (2000).

[4] A. G. Lebed, Phys. Rev. B **59**, R721 (1999); A. G. Lebed, K. Machida, and M. Ozaki, *ibid.* **62**, R795 (2000).

[5] C.-R. Hu, Phys. Rev. Lett. **72**, 1526 (1994).

[6] S. Kashiwaya and Y. Tanaka, Rep. Prog. Phys. **63**, 1641 (2000).

[7] K. Sengupta, I. Žutić, H.-J. Kwon, V. M. Yakovenko, and S. Das Sarma, Phys. Rev. B **63**, 144531 (2001).

[8] Y. Tanuma, K. Kuroki, Y. Tanaka, and S. Kashiwaya, Phys. Rev. B **64**, 214510 (2001); Y. Tanuma *et al.*, **66**, 094507 (2002).

[9] T. Löfwander, V. S. Shumeiko, and G. Wendin, Supercond. Sci. Technol. **14**, R53 (2001).

[10] Y. Tanaka, T. Hirai, K. Kusakabe, and S. Kashiwaya, Phys. Rev. B **60**, 6308 (1999).

[11] C. D. Vaccarella, R. D. Duncan, C. A. R. Sá de Melo, cond-mat/0302080.

[12] The current-phase relation $I \propto \sin(\phi/2)$ that we propose should not be confused with another unconventional current-phase relation $I \propto \sin(2\phi)$ with the period π, which was predicted theoretically for junctions between s- and d-wave superconductors [27, 28], s- and p-wave superconductors [27, 29], and for the $0°/45°$ junctions between two d-wave superconductors [30].

[13] Y. Tanaka and S. Kashiwaya, Phys. Rev. B **53**, 9371 (1996); R. A. Riedel and P. F. Bagwell, *ibid.* **57**, 6084 (1998); Yu. S. Barash, *ibid.* **61**, 678 (2000); Y. Tanaka and S. Kashiwaya, *ibid.* **56**, 892 (1997).

[14] A. Yu. Kitaev, cond-mat/0010440.

[15] A. M. Zagoskin, *Quantum Theory of Many-Body Systems* (Springer, New York, 1998).

[16] A. Furusaki, Superlattices Microstruct. **25**, 809 (1999).

[17] I. K. Yanson, V. M. Svistunov, and I. M. Dmitrenko, Sov. Phys. JETP **21**, 650 (1965).

[18] I. M. Dmitrenko and I. K. Yanson, JETP Lett. **2**, 154 (1965).

[19] D. N. Langenberg, D. J. Scalapino, B. N. Taylor, and R. E. Eck, Phys. Rev. Lett. **15**, 294 (1965).

[20] I. M. Dmitrenko, I. K. Yanson, and I. I. Yurchenko, Sov. Phys. Solid State **9**, 2889 (1968).

[21] A. K. Jain, K. K. Likharev, J. E. Lukens, and J. E. Savageau, Phys. Repts. **109**, 309 (1984).

[22] R. Kleiner, F. Steinmeyer, G. Kunkel, and P. Müller, Phys. Rev. Lett. **68**, 2394 (1992).

[23] R. F. Miracky, J. Clarke, and R. H. Koch, Phys. Rev. Lett. **50**, 856 (1983); C. B. Whan, C. J. Lobb, and M. G. Forrester, J. Appl. Phys. **77**, 382 (1995).

[24] E. A. Early, A. F. Clark, and K. Char, Appl. Phys. Lett. **62**, 3357 (1993); L. C. Ku *et al.*, Physica C **229**, 320 (1994); I. V. Borisenko *et al.*, Physica C **368**, 328 (2002).

[25] J. Clarke, Phys. Rev. Lett. **21**, 1566 (1968).

[26] E. Il'ichev *et al.*, Phys. Rev. Lett. **86**, 5369 (2001).

[27] S. Yip, J. Low T. Phys. **91**, 203 (1993).

[28] Y. Tanaka, Phys. Rev. Lett. **72**, 3871 (1994); A. M. Zagoskin, J. Phys. Condens. Matter **9**, L419 (1997).

[29] N. Yoshida, Y. Tanaka, S. Kashiwaya, and J. Inoue, J. Low T. Phys. **117**, 563 (1999).

[30] T. Löfwander, G. Johansson, M. Hurd, and G. Wendin, Phys. Rev. B **57**, R3225 (1998); M. Hurd, T. Löfwander, G. Johansson, and G. Wendin, *ibid.* **59**, 4412 (1999).